

# Quantum lifetimes and momentum relaxation of electrons and holes in Ga0.7In0.3N0.015As0.985/GaAs Quantum Wells

Mustafa Gunes, N. Balkan, Engin Tiras, Sukru Ardali, Chantal Fontaine, Alexandre Arnoult

▶ **To cite this version:**

Mustafa Gunes, N. Balkan, Engin Tiras, Sukru Ardali, Chantal Fontaine, et al.. Quantum lifetimes and momentum relaxation of electrons and holes in Ga0.7In0.3N0.015As0.985/GaAs Quantum Wells. Philosophical Magazine, 2010, pp.1. 10.1080/14786435.2010.525543 . hal-00639780

**HAL Id: hal-00639780**

**https://hal.archives-ouvertes.fr/hal-00639780**

Submitted on 10 Nov 2011

**HAL** is a multi-disciplinary open access archive for the deposit and dissemination of scientific research documents, whether they are published or not. The documents may come from teaching and research institutions in France or abroad, or from public or private research centers.

L'archive ouverte pluridisciplinaire **HAL**, est destinée au dépôt et à la diffusion de documents scientifiques de niveau recherche, publiés ou non, émanant des établissements d'enseignement et de recherche français ou étrangers, des laboratoires publics ou privés.




For Peer

# Quantum lifetimes and momentum relaxation of electrons and holes in Ga0.7In0.3N0.015As0.985/GaAs Quantum Wells

| | |
|---|---|
| Journal: | *Philosophical Magazine & Philosophical Magazine Letters* |
| Manuscript ID: | TPHM-10-Jul-0363.R2 |
| Journal Selection: | Philosophical Magazine |
| Date Submitted by the Author: | 16-Sep-2010 |
| Complete List of Authors: | Gunes, Mustafa; University of Essex, School of Computer Science and Electronic Engineering<br>Balkan, N.; Department of Computing and Electronic Systems, University of Essex, CO4 3SQ Colchester, United Kingdom<br>Tiras, Engin; Anadolu University, Physics<br>Ardali, Sukru; Anadolu University, Physics<br>Fontaine, Chantal; Laas-Cnrs<br>Arnoult, Alexandre; Laas-Cnrs |
| Keywords: | electrical transport, magnetoresistance, materials characterisation, mobility, semiconductors |
| Keywords (user supplied): | |

SCHOLARONE™
Manuscripts

# Quantum lifetimes and momentum relaxation of electrons and holes in $Ga_{0.7}In_{0.3}N_{0.015}As_{0.985}$/GaAs Quantum Wells

E. Tiras[a], N. Balkan[b*], S. Ardali[a], M. Gunes[b], C. Fontaine[c], and A. Arnoult[c]

[a] *Department of Physics, Faculty of Science, Anadolu University, Yunus Emre Campus, Eskisehir 26470, Turkey*
[b] *School of Computer Science and Electronic Engineering, University of Essex, Wivenhoe Park, Colchester CO4 3SQ, United Kingdom*
[c]*LAAS-CNRS 7 avenue du colonel Roche 31 077 - Toulouse Cedex 4 - France*

* Corresponding author's email: balkan@essex.ac.uk

*(Received XX Month Year; final version received XX Month Year)*

Electronic transport in n and p-type modulation-doped $Ga_{0.7}In_{0.3}N_{0.015}As_{0.985}$ /GaAs quantum wells are investigated using magneto-transport measurements in the temperature range between T=1.8 and 32 K and at magnetic fields up to B=11 T. The momentum relaxation and the quantum lifetimes ($\tau_q$) of electrons and holes are obtained directly from the temperature and magnetic field dependencies of the SdH oscillation amplitudes respectively. A detailed analysis of quantum and transport life times indicates that the momentum relaxation of holes is forward displaced in k-space whilst a large angle scattering mechanism is prominent for the electrons. This discrepancy is believed to be due to scattering of electrons with nitrogen complexes and to the lack of such a mechanism for holes.

Key words: GaInNAs, effective mass, quantum lifetime

For Peer Review Only

## 1. Introduction

Dilute nitrides, particularly the quaternary material system of GaInNAs/GaAs, have been attracting a great deal of attention because of their potential applications in a variety of optoelectronic devices [1-7]. Most of the work reported in the literature is concerned with the optical properties. However, studies of electronic transport, particularly in GaNAs, have also been reported [8-14].

It is predicted, theoretically, that the electron effective mass in GaInNAs is increased compared to that in the host matrix, GaInAs, as a result of reduced parabolicty, associated with nitrogen incorporation. The hole effective mass, however, is expected to remain unchanged [15, 16]. Previous experimental work has been concerned mainly with effective masses obtained indirectly from the analysis of transition energies [17-21], quantum confinement energy [22, 23], exciton diamagnetic shifts [22], magneto-photoluminescence [24] and energy-loss spectroscopy [25]. There are only a few experimental studies reported in the literature where the electron effective mass is obtained experimentally by direct methods, for example by using optically detected cyclotron resonance technique [26]. There are only a few experimental studies concerning the determination of hole effective mass [27-29]

In modulation doped 2-D III-V compounds, the Shubnikov-de Haas (SdH) effect has been proven to be a powerful tool for the determination of the in-plane effective mass m* and the quantum lifetime ($\tau_q$) of electrons [30, 31]. To our knowledge there is no such study in dilute nitrides to date. The aim of the current work is to determine directly the 2D in-plane electron and hole effective masses and quantum and transport lifetimes in modulation doped n and p type GaInNAs/GaAs quantum wells.

## 2. Experimental

The $Ga_{0.7}In_{0.3}N_{0.015}As_{0.985}$/GaAs quantum well samples were grown by the Molecular Beam Epitaxy (MBE) technique onto semi-insulating GaAs substrates and did not undergo either rapid or slow thermal annealing. The samples have three 7 nm wide $Ga_{0.7}In_{0.3}N_{0.015}As_{0.985}$ wells, separated by 50 nm wide GaAs barriers. The 40 nm central position of the barriers are doped (with Si for n-type, and with Be for p-type) and the





For Peer Review Only

remaining 5 nm on either side is undoped (spacer layers) as shown in Table1. For the transport measurements ohmic contacts were formed by using Au/Ge/In for the n- type and Zn/Au for the p-type material. Magneto-resistance measurements were carried on Hall-bar shaped samples as a function of both, temperature, in the range between $T$ =1.8 and 32 K, and magnetic field, in the range between B= 0 and 11 T, in a cryogen free superconducting magnet system (Cryogenics Ltd., Model no J2414). A constant current source (Keithley 2400) and a nano-voltmeter (Keithley 2182A) were employed in the conventional dc measurements. The current flow was in the plane of the electron gas and the current through the sample was kept low enough to ensure ohmic conditions. Steady magnetic fields were applied perpendicular to the plane of the samples.

## 3. Results and discussion

Figure 1 shows the magneto-resistance $R_{xx}(B)$ measured at different temperatures for both n and p-type modulation-doped $Ga_{1-x}In_xN_yAs_{1-y}$/GaAs quantum wells. SdH oscillations are clearly visible over the magnetic field range between B= 5 and 10 T. No higher harmonics are apparent in the oscillations and the oscillation amplitude is reduced with increasing temperature [32]. It is also evident that the oscillatory effect is superimposed on a monotonically increasing component, which occurs as a result of positive magneto-resistance in the barriers [33]. This may affect the accuracy of the determination of oscillation amplitude, particularly at elevated temperatures. Therefore, in order to exclude the effects of the background magneto-resistance ($R_b$) and to extract the SdH oscillations we used the negative second derivative of the raw magneto-resistance data with respect to the magnetic field, i.e. ($-\delta^2R/\delta B^2$) [30-33]. The oscillations in the second derivative of magneto-resistance have well defined envelopes and symmetrical about a horizontal line as shown at three different temperatures in figure 2. The double-differentiation technique does not change either the peak position or the period of the oscillations [33].

The period of the SdH oscillations has been obtained by plotting the reciprocal of magnetic field ($1/B_n$), at which the $n$th peak occurs, against the peak number ($n$).



http://mc.manuscriptcentral.com/pm-pml

For Peer Review Only

Provided that the carriers occupy only the lowest sub band, the plot of $1/B_n$ versus $n$ will be a straight line as we observe in figure 3. The slope of $1/B_n$ versus $n$ plot yields the oscillation period, $\Delta(1/B_n)$ and the 2D carrier density ($N_{2D}$) of each sample can be calculated using [31, 33]

$$\Delta\left(\frac{1}{B}\right)=\frac{e}{\pi\hbar N_{2D}}=\frac{e\hbar}{m^*\left(E_F-E_1\right)} \qquad (1)$$

where $E_F - E_1$ is the energy difference between the Fermi level and the bottom of the first subband. The results thus obtained for n and p type doped samples are n=2.68x$10^{12}$ $cm^{-2}$ and p=1.32x$10^{12}$ $cm^{-2}$, respectively. The carrier density is found to be essentially independent of temperature in the range from $T$=1.8 to 32 K.

The in-plane effective mass $m^*$ can be extracted from the temperature dependence of the SdH amplitude at constant magnetic field using [31-33].

$$\frac{A(T,B_n)}{A(T_0,B_n)}=\frac{T.\sinh\left(\frac{2\pi^2 k_B m^* T_0}{\hbar e B_n}\right)}{T_0.\sinh\left(\frac{2\pi^2 k_B m^* T}{\hbar e B_n}\right)} \qquad (2)$$

where $A(T,B_n)$ and $A(T_o,B_n)$ are the amplitudes of the oscillation peaks observed at a magnetic field $B_n$ and at temperatures $T$ and $T_o$, respectively. In the derivation of equation (2) the quantum lifetime of electrons is assumed to be independent of temperature [31, 35]. The relative amplitudes, $A(T,B_n)/A(T_o,B_n)$, are plotted in figure 4 for B=7.38 Tesla and B=8.3 Tesla for n and p type samples respectively. The relative amplitude decreases with increasing temperature as a result of the thermal damping [30, 36]. The in-plane effective mass of 2D electrons and holes are then determined by fitting the experimental data for the temperature dependence of $A(T,B_n)/A(T_o,B_n)$ to equation (2). We find $m_e^* = 0.084\,m_0$ and $m_h^* = 0.155\,m_0$. We obtained similar values for all the magnetic fields of measurements suggesting strongly that the in-plane effective mass is essentially independent of magnetic field.





For Peer Review Only

Our electron effective mass for the n-type modulation-doped $Ga_{0.7}In_{0.3}N_{0.015}As_{0.985}$ /GaAs quantum wells agree extremely well with those obtained for the same nitrogen mole fraction by *Heroux et al.* [6] and *Tomic* and *O'Reilly* [16]. As for the hole effective mass, our result for the p-type modulation-doped $Ga_{0.7}In_{0.3}N_{0.015}As_{0.985}$/GaAs quantum wells are higher than the theoretically estimated values by *Wartak* and *Weetman* [27, 28] and our theoretical and experimental results that are obtained by using optical transition energies [34]. This might be the result of heavy and light hole band mixing in p- type material and the involvement of both heavy and light holes in the SdH oscillations. It is worth noting that the SdH oscillation peaks in p-modulation doped material are broader than those in the n-modulation doped sample which might be explained in terms of strain induced band mixing in the valence band. Indeed our observed effective hole mass is close to the range of values quoted for the heavy and light hole masses obtained by using time-resolved and magneto-photoluminescence spectroscopy by *Polimeni et al.* [29].

The Fermi energies for the samples obtained from the oscillation period using equation (1) together with the in-plane effective mass $m^*$ of 2D carriers are: $E_F$-$E_1$=75.6 meV and 36.0 meV for the n and p type samples respectively. The quantum lifetime ($\tau_q$) can be determined from the magnetic-field dependence of the amplitude of the SdH oscillations (i.e. Dingle plots) at a constant temperature provided that the carrier effective mass is known [31, 33, 36]. Figure 5 shows typical plots for the Dingle plots for the samples investigated. There agreement is excellent between the experimental data and the straight line described by [31, 36], i.e.

$$ln\left[\frac{A(T,B_n).B_n^{-1/2}.\sinh\chi}{\chi}\right]=C-\frac{\pi m^*}{e\tau_q}\frac{1}{B_n}\ , \qquad (3)$$

where $\chi = 2\pi^2 k_B T/(\hbar\omega_c)$, $\omega_C(=eB_n/m^*)$ is the cyclotron frequency and $C$ is a constant. The quantum lifetimes, obtained from the slope of the Dingle plot using equation (3) together with the measured values of $m^*$, are $\tau_q$=0.051 ps and $\tau_q$=0.218 ps for electrons and holes, respectively. These values remain constant within 2 % in the whole temperature and magnetic-field ranges of the measurements. The quantum lifetime and



http://mc.manuscriptcentral.com/pm-pml

For Peer Review Only

quantum mobility ( $\mu_q = e\frac{\tau_q}{m^*}$ ) for both electrons and holes are tabulated together with the transport lifetime and transport (Hall) mobility ( $\mu_{tr} = e\frac{\tau_{tr}}{m^*}$ ) in table 2.

Transport mobility in the n and p -modulation doped samples is determined, in the ohmic regime, from the Hall measurements at liquid helium temperatures for the n and p type doped samples, $\mu_e$ = 1100 cm$^2$/Vs and $\mu_h$ = 3125 cm$^2$ / Vs respectively [34] are also shown in table 2. Using the experimentally determine effective mass together with the classical Hall mobility expression the transport lifetime $\tau_{tr}$ for electrons and holes as 0.043 ps and 0.275 ps, respectively. It is worth noting that both the quantum and transport lifetimes of holes much higher than that of electrons. The transport -to- quantum lifetime ratios of electrons is $\tau_{tr}/\tau_q$ ~ 0.8 ; while the transport-to-quantum lifetime ratios of holes is $\tau_{tr}/\tau_q$ ~1.3 .Theoretical calculations relating the transport lifetime to the quantum lifetime predict, in the extreme quantum limit, a $\tau_t/\tau_q$ ratio greater than unity for small-angle scattering and smaller than unity for large-angle scattering [31, 34, 37]. This implies that in our p-type sample where $\tau_{tr}/\tau_q$ ~ 1.3 the scattering of holes are mainly forward displaced in momentum space, which is in agreement with the model where the Hall mobility at low temperatures is limited by the interface roughness scattering [34]. In the n-type sample where $\tau_{tr}/\tau_q$ ~ 0.8 the dominant electron scattering is large-angle scattering. This may be expected from scattering of electrons with higher mass nitrogen complexes that occupy states below and above the conduction band [34]. Furthermore, it is evident from table 2 that both the low temperature Hall and the quantum mobilities of holes are significantly larger than electron mobilities suggesting that electrons in the conduction band experience an extra scattering compared to the holes, in accord with models based on scattering with nitrogen complexes occupying states below the conduction band [37, 38].

In order to determine whether the observed difference in the electron and hole mobilities is intrinsic and associated with the disparity in their effective masses we carried out a detailed modelling of the $Ga_xIn_{1-x}N_yAs_{1-y}$ conduction (CB) and valence band (VB) structures. The band structure of $Ga_xIn_{1-x}N_yAs_{1-y}$/GaAs QWs is calculated by solving the





For Peer Review Only

modified 8-band **k.p** Lüttinger-Kohn Hamiltonian, including tetragonal strain and strong coupling between the GaInAs CB and the localized nitrogen levels. The eigenvalue problem is then solved by the transfer-matrix method, taking into account the interfacial discontinuity condition [39, 40]. The valence band material parameters used for the calculations are the ones of GaInAs [34-41]. As far as the CB is concerned, the energy level of nitrogen ( $E_N$ ) is assumed to be constant relative to the vacuum level. Moreover, the coupling parameter in band anticrossing model (BAC), $V_{NM}$ has been taken as dependent on both In and N compositions. The details of theoretical model used in this work is given elsewhere [34] and only calculated effective mass of carriers lying band edge for e1 and hh1 level in the GaInNAs quantum well are tabulated in table 2. The calculation indicates that the presence of nitrogen induces strong perturbation mainly on the conduction states by mutual repulsion between the CB-edge state and localized N states leading to enhanced non-parabolicity of CB in GaInNAs. Therefore, the electron effective mass is much higher in GaInNAs ( $m_e^* = 0.084\, m_0$ ) than the nitrogen free material GaInAs ( $m_e^* = 0.054 m_0$ ) [34]. However, the nitrogen incorporation has negligible effect on the valence band (VB), thus the calculated hole effective mass ( $m_h^* = 0.105\, m_0$ ) is independent of nitrogen in the composition [34]. In addition, the nitrogen induces the flattening of the lower sub-band, giving rise to an enhanced density of states of electron at CB edge. Therefore, the density of electrons is expected to be higher than that of holes in the GaInNAs QWs with same nitrogen concentration as depicted in table 2.

## 4. Conclusions

The carrier density ($N_{2D}$), effective mass ($m^*$), and quantum lifetime ($\tau_q$) for electrons and holes in n and p-type modulation-doped $Ga_{1-x}In_xN_yAs_{1-y}$/GaAs quantum wells have been determined from SdH oscillations. The two-dimensional (2D) carrier density and the Fermi energy with respect to subband energy ($E_F - E_1$) have been obtained from the periods of the SdH oscillations. The in-plane effective mass (m*) and the quantum lifetime ($\tau_q$) of electrons have been extracted from the temperature and magnetic field dependencies of the SdH amplitude, respectively. The in-plane effective



http://mc.manuscriptcentral.com/pm-pml

For Peer Review Only

mass of electrons and holes at their measured Fermi energies are $0.084m_0$ and $0.155m_0$ respectively. The quantum life time for electrons and holes in our n and p-type modulation doped quantum wells are 0.051ps and 0.218ps respectively. A detailed analysis of the quantum and transport life times indicates strongly that the momentum relaxation of holes are forward displaced in k-space where large angle scattering is prominent for the electrons. This discrepancy is believed to be due to scattering of electrons with nitrogen complexes.

**Acknowledgments**

E. TIRAS is grateful to the Scientific and Technical Research Council of Turkey TUBITAK (Project no: 110T377) and Anadolu University (Project no: 091047) for their financial support. We also acknowledge the support of COST Action: MP0805 for providing the suitable platform for the successful execution of the research.

**References**

[1] J.S. Harris, Semicond. Sci. Technol. 17 (2002) p. 880.

[2] D.B. Jackrel, S.R. Bank, H.B. Yuen, M.A. Wistey, J.S. Harris, A.J. Ptak, S.W. Johnston, D.J. Friedman, S.R. Kurtz, J. Appl. Phys. 101 (2007) p. 114916.

[3] P.C. Chang, A.G. Baca, N.Y. Li, P.R. Sharps, H.Q. Hou, J.R. Laroche, F. Ren, Appl. Phys. Lett. 76 (2000) p. 2788.

[4] S. Calvez, J-M Hopkins, S.A. Smith, A.H. Clark, R. Macaluso, H.D. Sun, M.D. Dawson, T. Jouhti, M. Pessa, K. Gundogdu, K.C. Hall, T.F. Boggess, J. Cryst. Growth 268 (2004) p. 457.

[5] J.O. Mitomo, M. Yokozeki, Y. Sato, Y. Hirano, T. Hino, H.Narui, IEEE J. Selected Topics in Quant. Electron. 11 (2005) p. 1099.

[6] J.B. Heroux, X. Yang, W.I. Wang, Appl. Phys. Lett. 75 (1999) p. 2716.

[7] J.F. Geisz and D.J. Friedman. Semicond. Sci. Technol. 17 (2002) p.769.

[8] Y. Sun, N. Balkan, A. Erol, M.C. Arikan, Microelectron. J. 40 (2009) p. 403.



For Peer Review Only

[9] R.J. Potter, N. Balkan, J. Phys.: Condens. Matter, 16 (2004) p. 3387.

[10] X.D. Luo, Z.Y. Xu, W.K. Ge, Z. Pan, L.H. Li, Y.W. Lin, Appl. Phys. Lett. 79 (2001) p. 958.

[11] I. J. Fritz, T. J. Drummond, G. C. Osbourn, J. E. Schirber, E. D. Jones, Appl. Phys. Lett. 48 (1986) p. 1678.

[12] T. Matsuoka, E. Kobayashi, K. Taniguchi, C. Hamaguchi, S. Sasa, Jpn. J. Appl. Phys. 29 (1990) p.2017.

[13] R. Mouillet, L. A. de Vaulchier, E. Deleporte, Y. Guldner, L. Travers and J. C. Harmand, Solid State Commun. 126 (2003) p. 333.

[14] D. Fowler, O. Makarovsky, A. Patanè, and L. Eaves, Phys. Rev. B 69 (2004) p. 153305.

[15] C. Skierbiszewski, P. Perlin, P. Wisniewski, T. Suski, W. Walukiewicz, W. Shan, J. W. Ager, E. E. Haller, J. F. Geisz, D. J. Freidman, J. M. Olson, and S. R. Kurtz, Phys. Status Solidi B 216 (1999) p.135.

[16] S. Tomic and E.P. O'Reilly, Phys. Rev. B 71 (2005) p. 233301.

[17] M. Hetterich, M. D. Dawson, A. Yu. Egorov, D. Bernklau, and H. Riechert, Appl. Phys. Lett. 76 (2000) p. 1030.

[18] Z. Pan, L. H. Li, Y. W. Lin, B. Q. Sun, D. S. Jiang, and W. K. Ge, Appl. Phys. Lett. 78 (2001) p. 2217.

[19] J.Y. Duboz, J. A. Gupta, M. Byloss, G. C. Aers, H. C. Liu, and Z. R. Wasilewski, Appl. Phys. Lett. 81 (2002) p. 1836.

[20] J. B. Héroux, X. Yang, and W. I. Wang, J. Appl. Phys. 92 (2002) p. 4361.

[21] C. Skierbiszewski, P. Perlin, P. Wisniewski, W. Knap, T. Suski, W. Walukiewicz, W. Shan, K. M. Yu, J. W. Ager, E. E. Haller, J. F. Geisz, J. M. Olson, Appl. Phys. Lett. 76 (2000) p. 2409.

[22] E. D. Jones, N. A. Modine, A. A. Allerman, I. J. Fritz, S. R. Kurtz, A. F. Wright, S. T. Tozer, and X. Wei, Proc. SPIE 3621 (1999) p.52.

[23] Y. Zhang, A. Mascarenhas, H. P. Xin, and C. W. Tu, Phys. Rev. B 61 (2000)p. 7479.

[24] G. Baldassarri Höger von Högersthal, A. Polimeni, F. Masia, M. Bissiri, M. Capizzi, D. Gollub, M. Fischer, and A. Forchel, Phys. Rev. B 67 (2003) p. 233304.

For Peer Review Only

[25] M.H. Gass, A. J. Papworth, T. B. Joyce, T. J. Bullough, and P. R. Chalker, Appl. Phys. Lett. 84 (2004) p. 1453.

[26] P. N. Hai, W. M. Chen, I. A. Buyanova,H. P. Xin, C. W. Tu, Appl. Phys. Lett. 77 (2000) p.1843.

[27] M.S. Wartak, P. Weetman, J. Phys.: Condens. Matter 17 (2005) p.6539.

[28] M.S. Wartak, P. Weetman, J. Phys.: Condens. Matter 19 (2007) p. 276202.

[29] A. Polimeni, F. Masia, A. Vinattieri, G. Baldassarri Hoger von Hogersthal and M. Capizzi, Appl. Phys. Lett 84 (2004) p. 2295.

[30] N. Balkan, H. Celik, A.J. Vickers and M. Cankurtaran, Phys. Rev. B 52 (1995) p. 210.

[31] E. Tiras, M. Cankurtaran, H. Çelik, A. Boland Thoms, N. Balkan, Superlattices and Microstruct. 29 (2001) p. 147.

[32] D.G. Seiler and A.E. Stephens, *Landau Level Spectroscopy*, G Landwehr and E I Rashba eds., Amsterdam: North-Holland, *V*ol 2 1991 p. 1031.

[33] S.B. Lisesivdin, N. Balkan, O. Makarovsky, A. Patane, A. Yildiz, M.D. Caliskan, M. Kasap, S. Ozcelik, E. Ozbay, J. Appl. Phys. 105 (2009) p. 093701.

[34] Y. Sun, N. Balkan, M. Aslan, S. B. Lisesivdin, H. Carrere, M. C. Arikan, X. Marie, J. Phys.: Condens. Matter 21 (2009) p. 174210.

[35] H. Celik, M. Cankurtaran, A. Bayrakli, E. Tiras and N. Balkan, Phys. Status Solidi B 207 (1998) p. 139.

[36] H. Celik, M. Cankurtaran, A. Bayrakli, E. Tiras, and N. Balkan, Semicond. Sci. Technol. 12 (1997) p. 389.

[37] A. Polimeni, F. Masia, G. Pettinari, R. Trotta, M. Felici, M. Capizzi, A. Lindsay, E. P O'Reilly, T. Niebling, W. Stolz, P. J. Klar, Phys. Rev. B 77 (2008) p. 1552.

[38] A. Lindsay, E. P. O'Reilly, A. D. Andreev, T. Ashley, Phys. Rev. B 77 (2008) p. 165205.

[39] P. T. Coleridge, Phys. Rev. B 44 (1991) p. 3793.

[40] H. Carrère, V.G. Truong, X. Marie, T. Amand, B. Urbaszek, R. Brenot, F. Lelarge, and B. Rousseau, Microelectron. J. 40 (2009) p. 827.

[41] I. Vurgaftman, J. R. Meyer and L. R. Ram-Mohan, Appl. Phys. Rev. 89 (2001) p. 5815.



For Peer Review Only

Table 1. The structure of the n and p-type modulation-doped $Ga_{1-x}In_xN_yAs_{1-y}$/GaAs quantum wells sample used in the studies.

| **Material** | **Thickness** (nm) | **Doping** ($cm^{-3}$) | |
|---|---|---|---|
| GaAs (Cap) | 50 | Si (n)/Be (p): $1x10^{18}$ | |
| GaAs (Barrier) | 20 | Si (n)/Be (p): $1x10^{18}$ | x3 |
| GaAs (Spacer) | 5 | Undoped | |
| $Ga_{1-x}In_xN_yAs_{1-y}$ QW | 7 | Undoped | |
| GaAs(Spacer) | 5 | Undoped | |
| GaAs(Barrier) | 20 | Si (n)/Be (p): $1x10^{18}$ | |
| GaAs (Buffer) | 50 | Undoped | |
| Semi insulating GaAs Substrate | | | |

For Peer Review Only

Table 2. Effective mass, transport and quantum lifetimes and mobilities for holes and electrons

| **Sample (Doping)** | **2D carrier density $cm^{-2}$** | **Fermi level (from The first subband)** | **Effective mass (Experiment)** | **Effective mass (Theory)** | **Quantum lifetime $\tau_q$** | **Transport lifetime $\tau_{tr}$** | **Quantum mobility $\mu_q(cm^2/Vs)$** | **Transport mobility $\mu_{tr}(cm^2/Vs)$** |
|---|---|---|---|---|---|---|---|---|
| **1930**: $Ga_{0.7}In_{0.3}N_{0.015}As_{0.985}$ (n) | $n=2.68x10^{12}$ | 75.6 meV | $m_e^*=0.084m_0$ | $m_e^*=0.080m_0$ | 0.051ps | 0.043 ps | 1067 | 1100 |
| **1931:** $Ga_{0.7}In_{0.3}N_{0.015}As_{0.985}$ (p) | $p=1.32x10^{12}$ | 36.0 meV | $m_h^*=0.155m_0$ | $m_h^*=0.105m_0$ | 0.218ps | 0.275 ps | 2473 | 3125 |

For Peer Review Only

**Figure Captions**

Figure 1. Magneto-resistance ($R_{xx}$) as a function of magnetic field both (a) n and (b) p-type modulation-doped $Ga_{0.7}In_{0.3}N_{0.015}As_{0.985}$/GaAs quantum wells measured at different temperatures.

Figure 2. The second derivative of magneto-resistance with respect to magnetic field plotted against the magnetic field. The double differentiation removes the background magneto-resistance without affecting the position and the amplitudes of the oscillatory component.

Figure 3. The reciprocal magnetic field ($1/B_n$) plotted as a function of the oscillation peak number. The straight line is the least-squares fit to the experimental data and the circles, squares and triangles symbols correspond to the peak magnetic field data for (a) n and (b) p-type modulation-doped samples measured at three different temperatures.

Figure 4. Temperature dependence of the normalized amplitude of the oscillation peak at a fixed magnetic field of ($B_n$) measured for (a) n and (b) p-type modulation-doped samples. The data points are represented by the full circles. The full curves are the best fits of equation (2) to the experimental data.

Figure 5. Determination of the quantum lifetime for (a) n and (b) p-type modulation-doped samples. The data points are represented by the full squares. The straight lines are the least-squares fits of equation (3) to each set of the experimental data.

For Peer Review Only

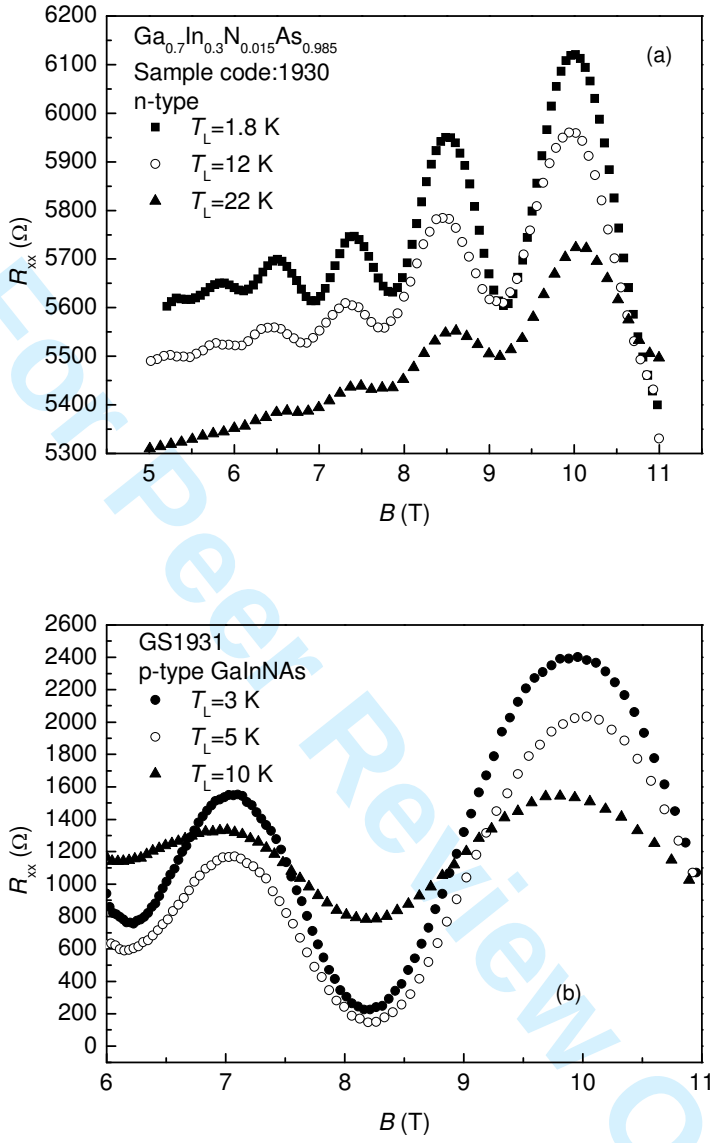


**Figure 1.**

For Peer Review Only

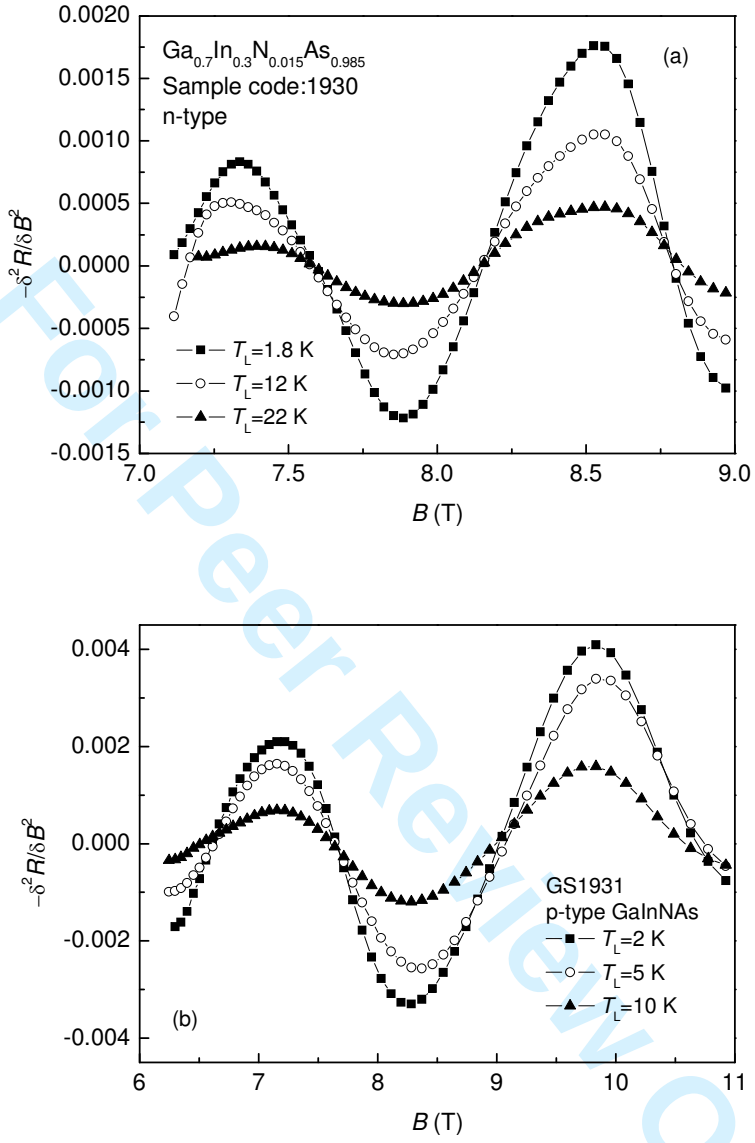


**Figure 2**

For Peer Review Only

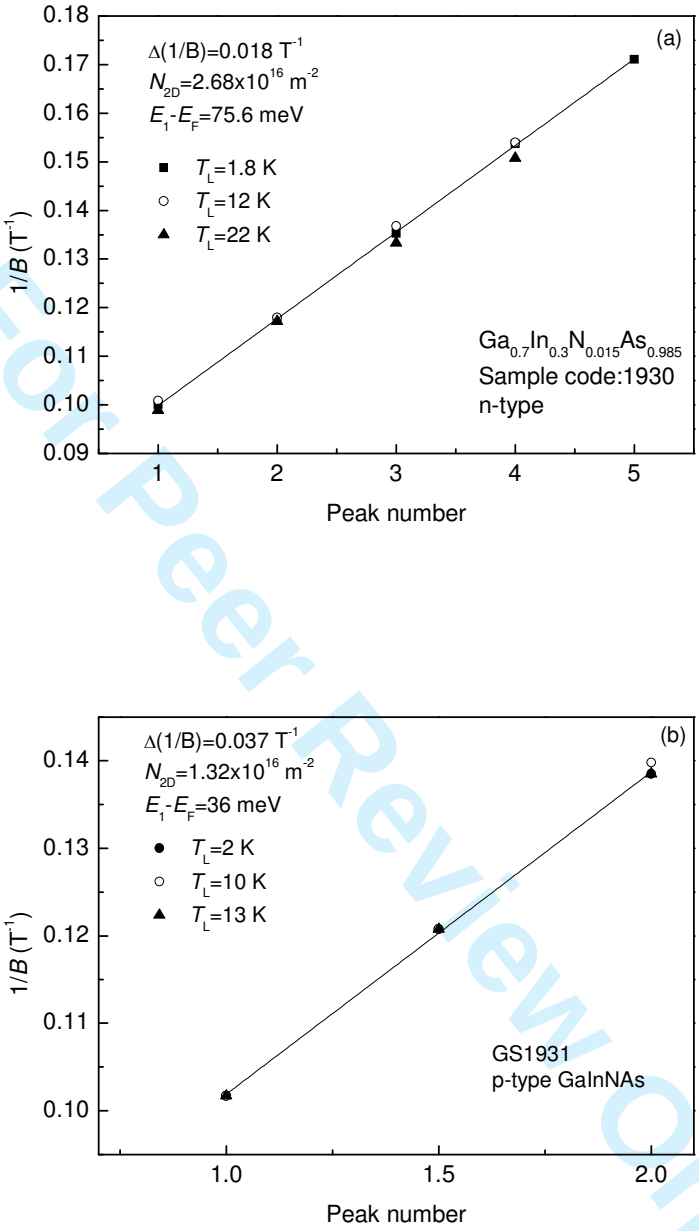


**Figure 3**

For Peer Review Only

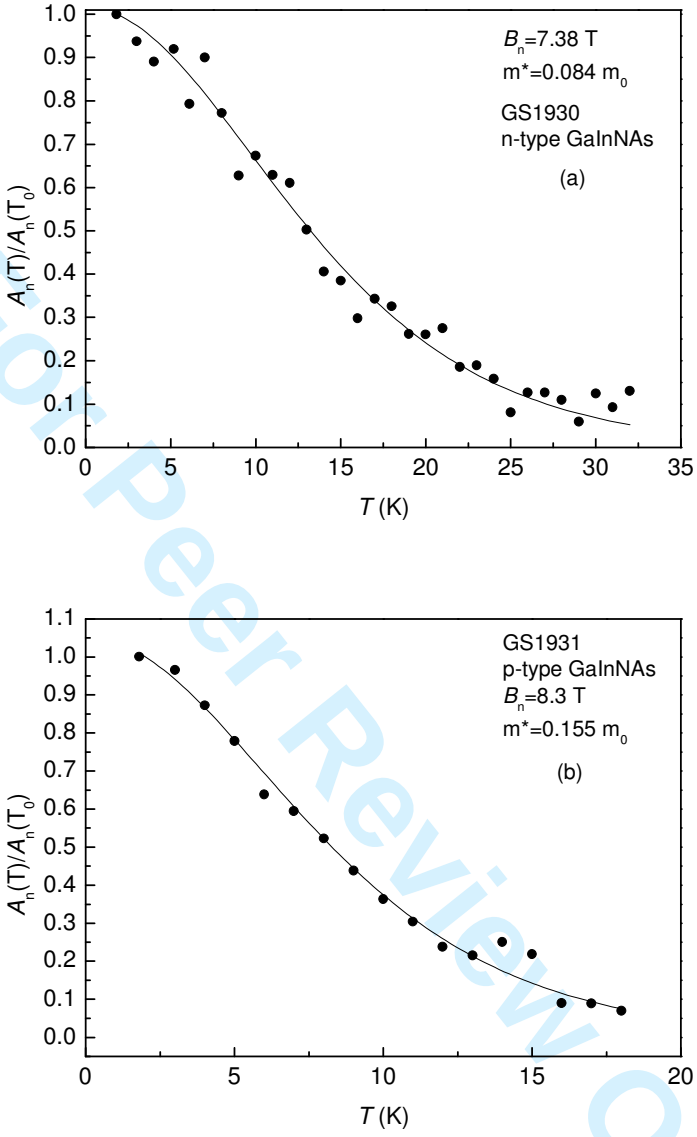


**Figure 4**

For Peer Review Only

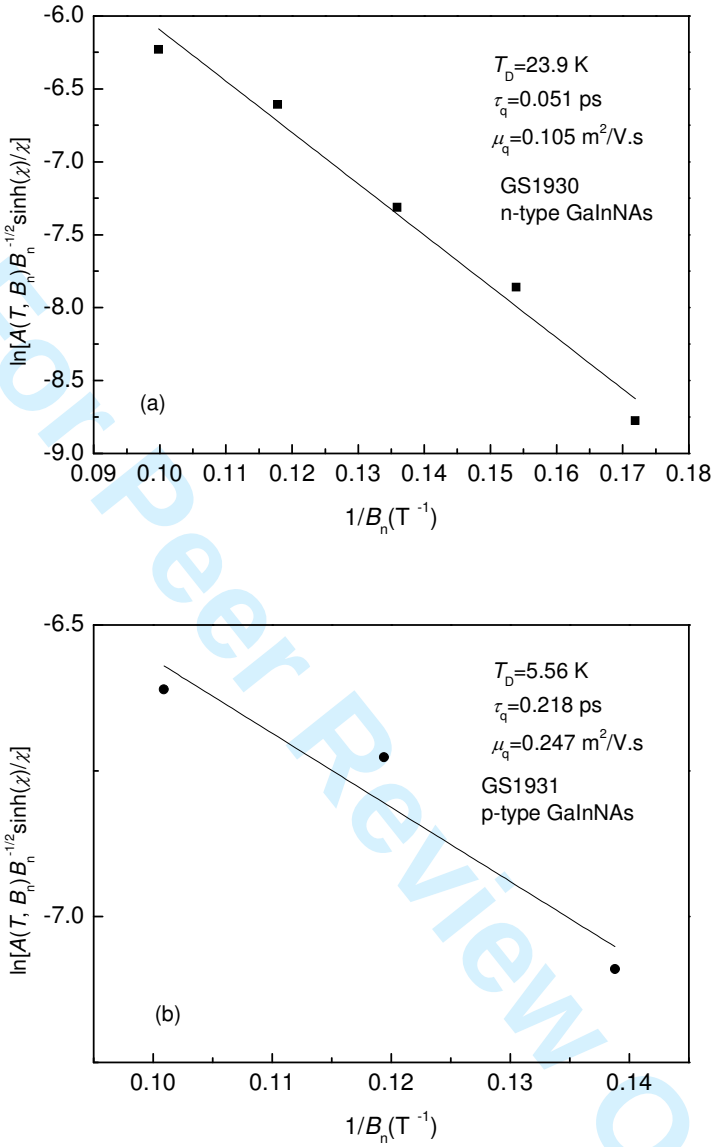


**Figure 5**

For Peer Review Only

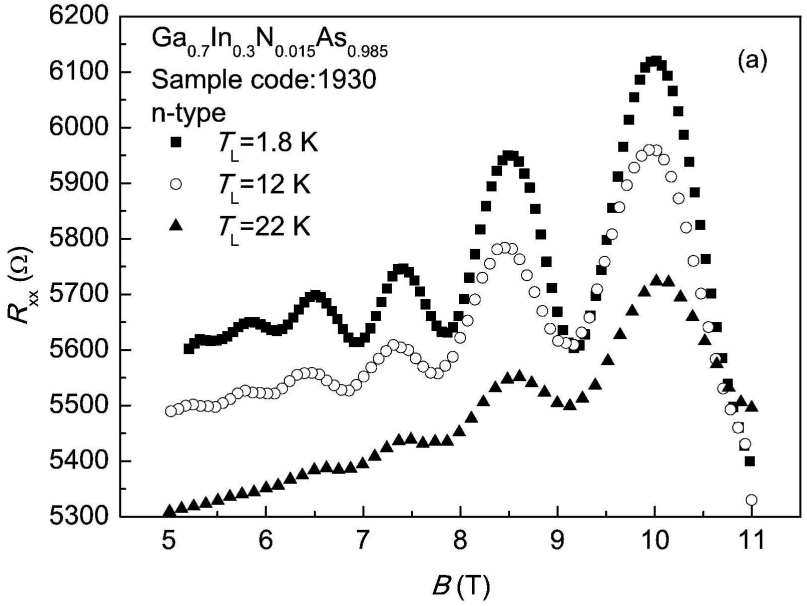


253x177mm (600 x 600 DPI)

For Review Only

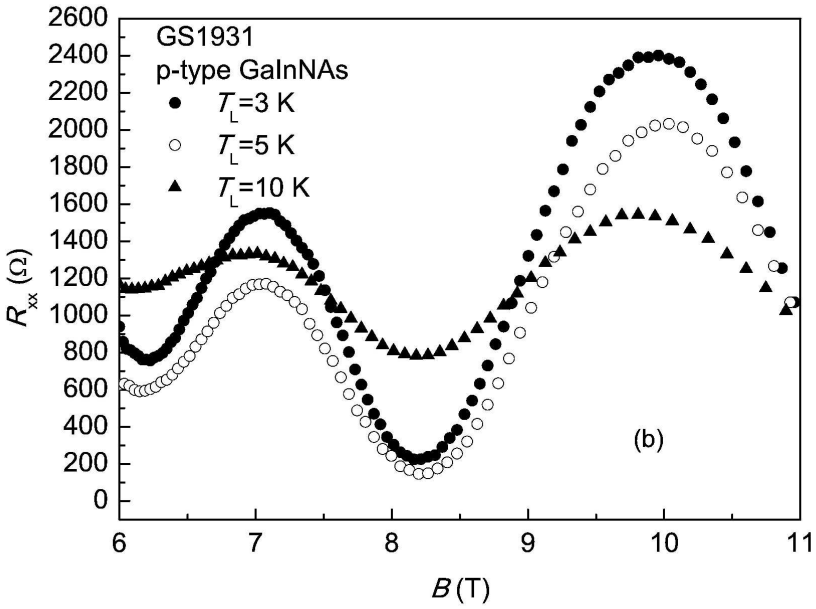


253x177mm (600 x 600 DPI)

For Peer Review Only

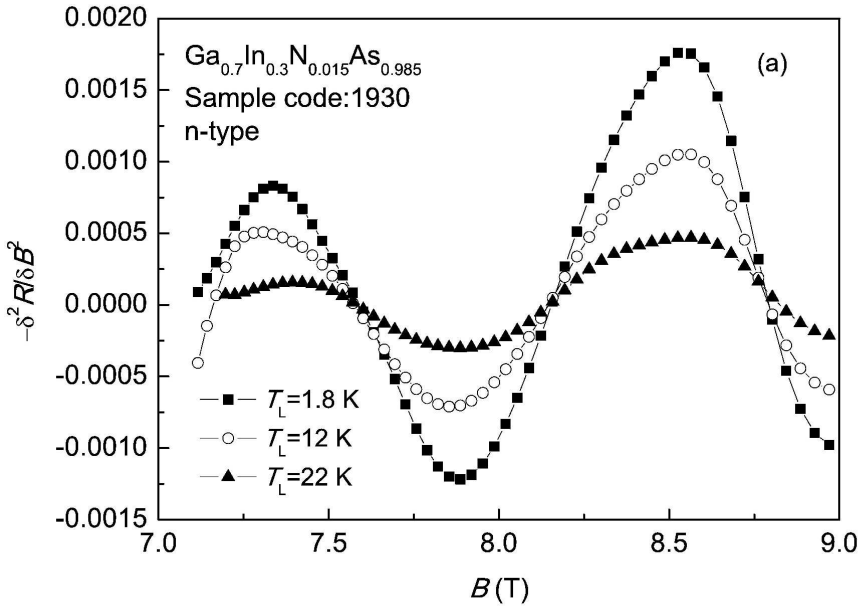


253x177mm (600 x 600 DPI)

For Peer Review Only

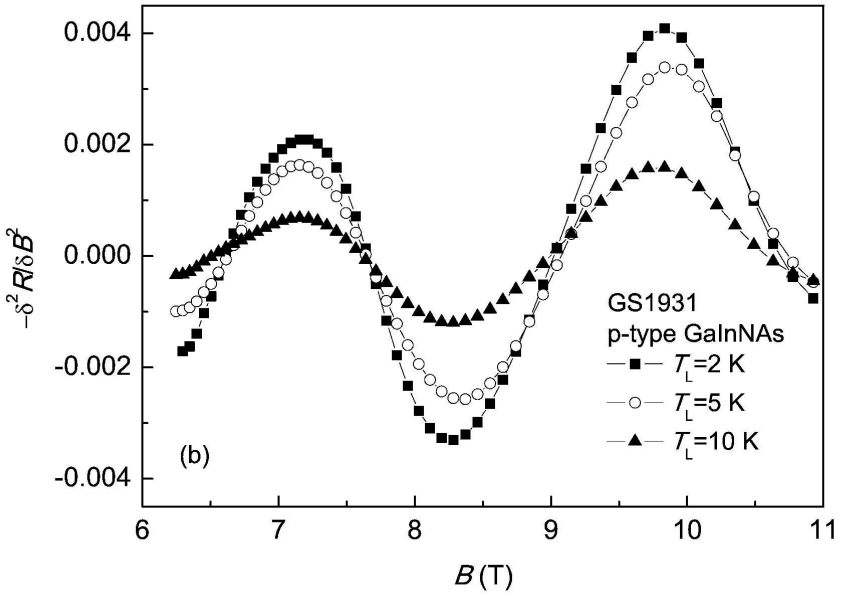


253x177mm (600 x 600 DPI)

View Only

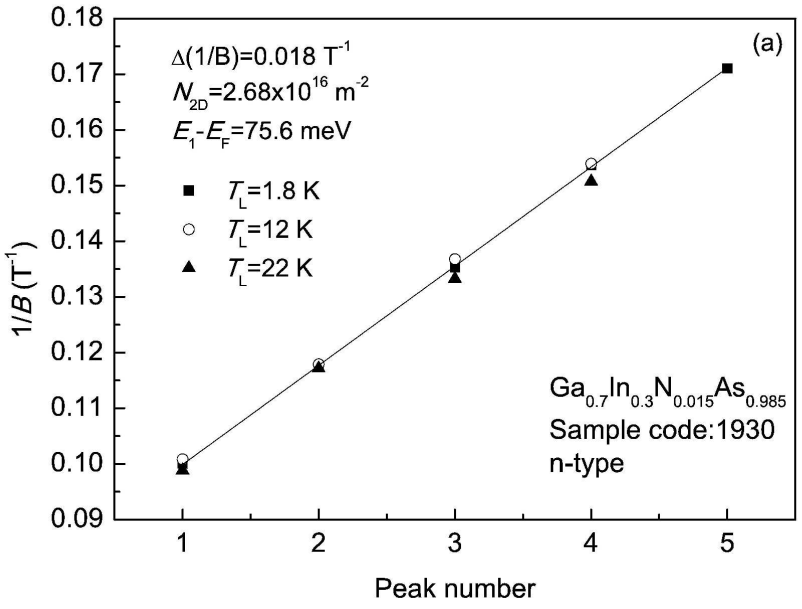


253x177mm (600 x 600 DPI)

View Only

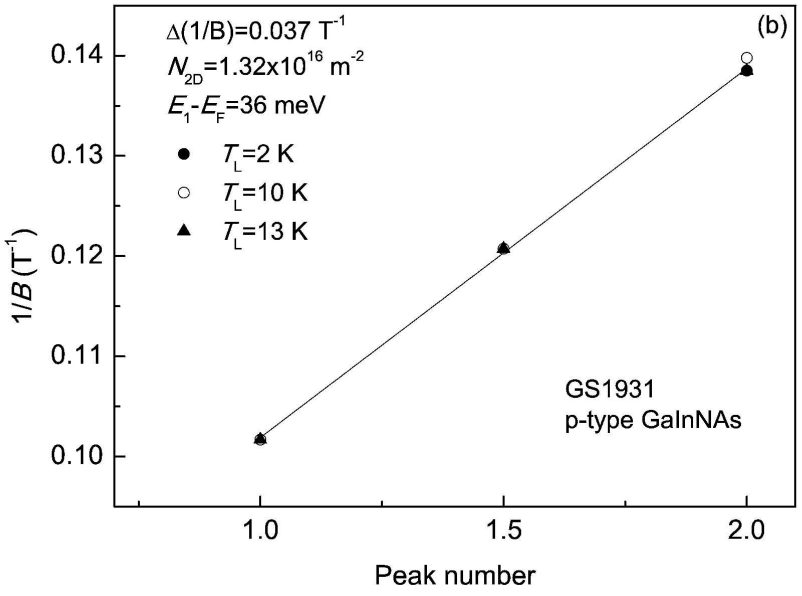


253x177mm (600 x 600 DPI)

View Only

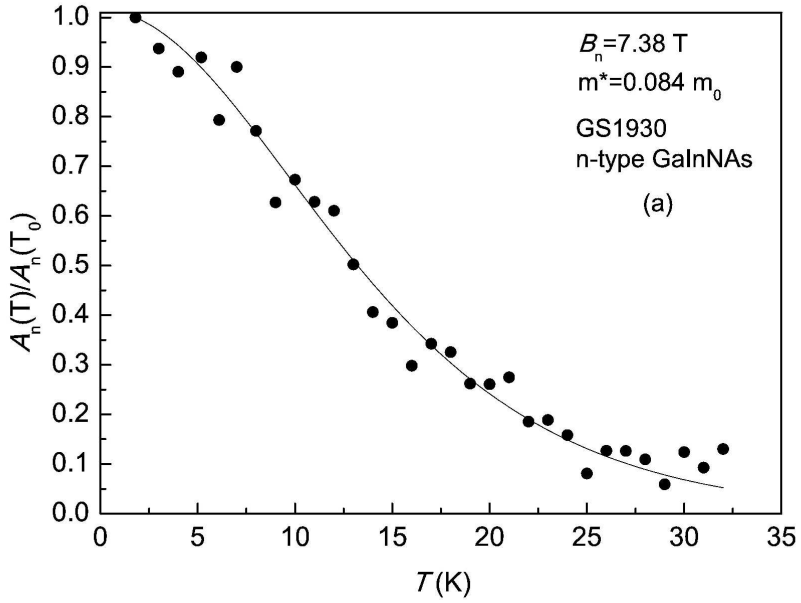


253x177mm (600 x 600 DPI)

For Peer Review Only

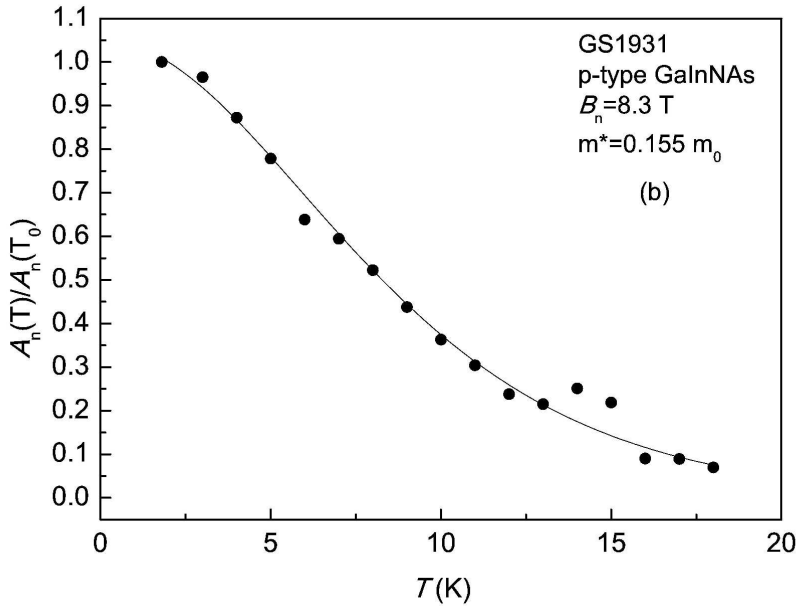


253x177mm (600 x 600 DPI)

For Peer Review Only

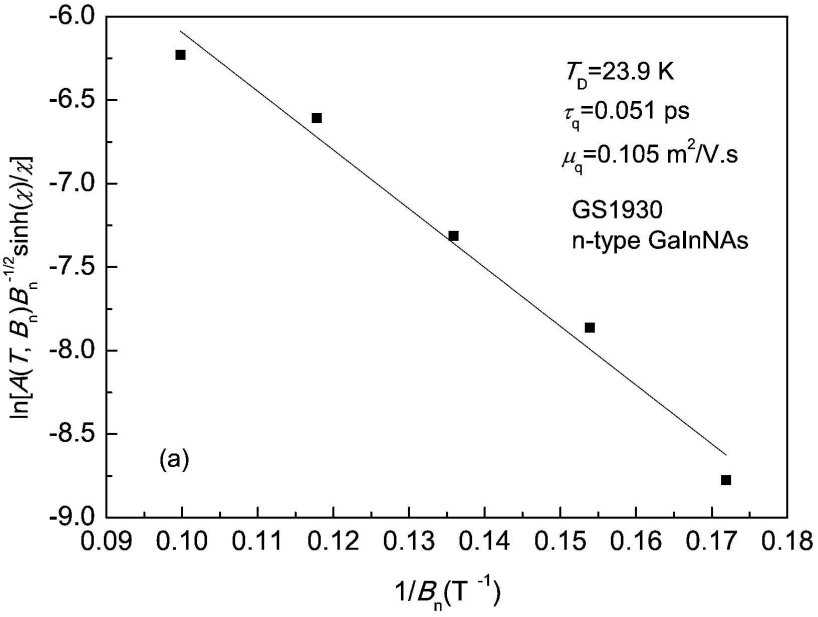


253x177mm (600 x 600 DPI)

View Only

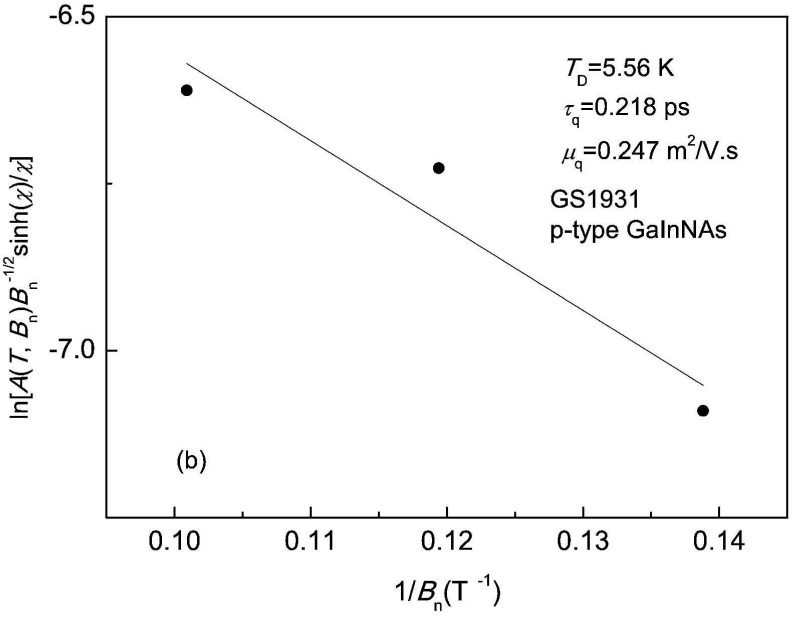


253x177mm (600 x 600 DPI)

View Only